ACS OMEGA

Open Access

http://pubs.acs.org/journal/acsodf

Article

Insights into Novel Arylazopyrazolo[1,5-*a*]pyrimidines as Promising MurA Inhibitors and Antibiofilm Candidates: Design, Synthesis, Antimicrobial Evaluation, and Molecular Docking

Omkulthom Al kamaly, Amel S. Younes, Mona H. Ibrahim, Marwa F. Harras,* Aisha A. Alsfouk, and Rehab Sabour

Cite This: *ACS Omega* 2025, 10, 4044−4056

Read Online

ACCESS | Metrics & More | Article Recommendations | Supporting Information

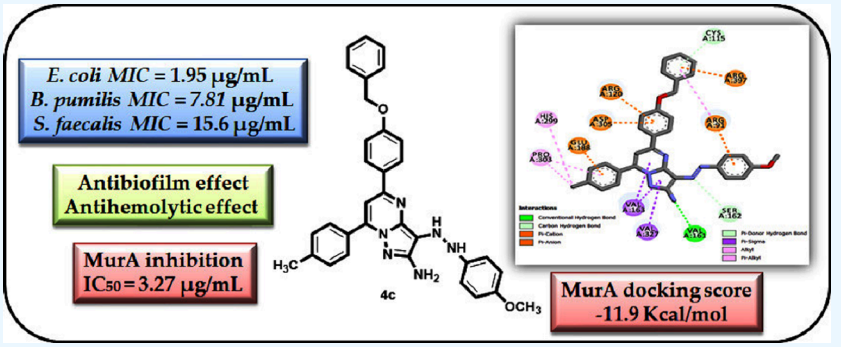

ABSTRACT: MurA is a pivotal target in antimicrobial therapy owing to its fundamental function in bacterial cell wall production; inhibiting this enzyme not only disrupts cell integrity, leading to bacterial lysis, but also presents a promising strategy to combat the growing threat of antibiotic resistance by providing an effective approach to both G+ve and G-ve microorganisms. Novel pyrazolo[1,5-*a*]pyrimidine derivatives are produced and measured for their antibacterial effectiveness. Based on the acquired findings, a majority of the examined compounds exhibited encouraging antibacterial characteristics. Among the examined compounds, **4c** emerged as a standout candidate, exhibiting (MIC) = 1.95 μg/mL against *Escherichia coli* and demonstrating significant potency as a MurA inhibitor with (IC_{50}) of 3.77 ± 0.2 μg/mL, comparable to the established antibiotic fosfomycin. Additionally, compound **4c** displayed an impressive antibiofilm activity against multiple microorganisms, indicating its potential to combat biofilm-related infections. The compound also reduced hemolysis percentage, suggesting a strong antihemolytic effect. Molecular docking studies confirm that **4c** engages in crucial residues within the MurA active site, elucidating its mechanism of action.

1. INTRODUCTION

The development of novel antibiotics has become increasingly crucial since the mid-1900s, when resistant strains of bacteria first appeared. A multitude of strategies have been employed to develop therapeutic drugs featuring innovative chemical scaffolds and distinctive modes of action in response to such resistance.[1] Given that bacteria are resistant to β-lactam antibiotics and there is an urgent necessity to discover new antibacterial agents, drug development initiatives have redirected focus toward less investigated strategies within the peptidoglycan manufacturing pathway. With the assistance of the Mur enzymes (Mur A-F), this work sought to examine the early cytoplasmic phases of peptidoglycan synthesis. The primary peptidoglycan precursor, uridine-5-diphosphate-*N*-acetylmuramyl-pentapeptide, is synthesized with the aid of Mur enzymes. As a result, Mur enzymes are thought to be promising prospects for drug discovery.[2] Peptidoglycan as an essential component of G+ve and G-ve bacteria's cell walls give cells shape and afford protection from being destroyed by osmotic pressure. The ability to generate effective antibacterial agents by interfering with the bacterial cell wall production is well documented. Several clinically significant antibacterial agents specifically block enzymes that contribute to the steps of cell wall production that entail cross-linking; therefore, one approach that shows promise for developing new antibacterial drugs is to concentrate on the biosynthetic mechanisms involved in cell wall building.[3,4] The initial phase of cell wall biosynthesis is catalyzed by MurA enzyme, which allows

Received: November 12, 2024
Revised: January 7, 2025
Accepted: January 14, 2025
Published: January 24, 2025

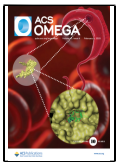

https://doi.org/10.1021/acsomega.4c10286
ACS Omega 2025, 10, 4044−4056

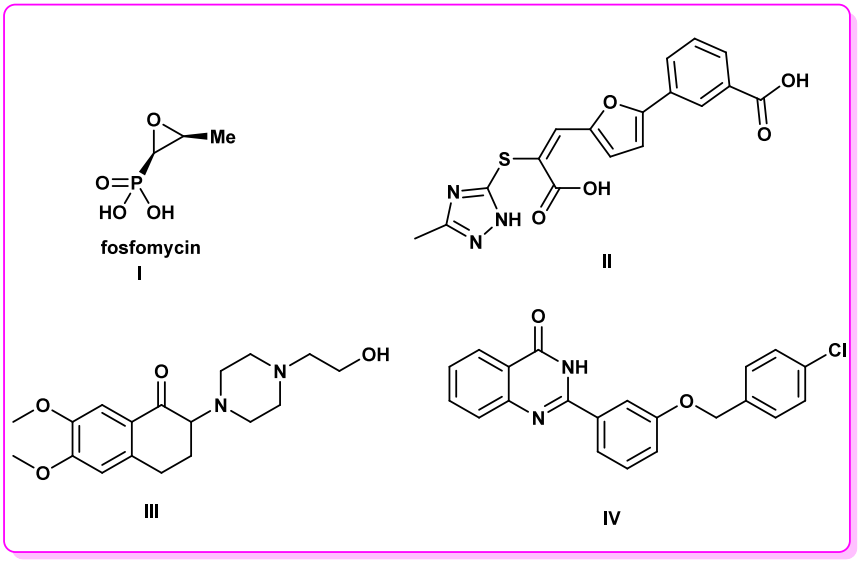

Figure 1. Fosfomycin (**I**) and some reported MurA inhibitors (**II**–**IV**) of different chemical structures.

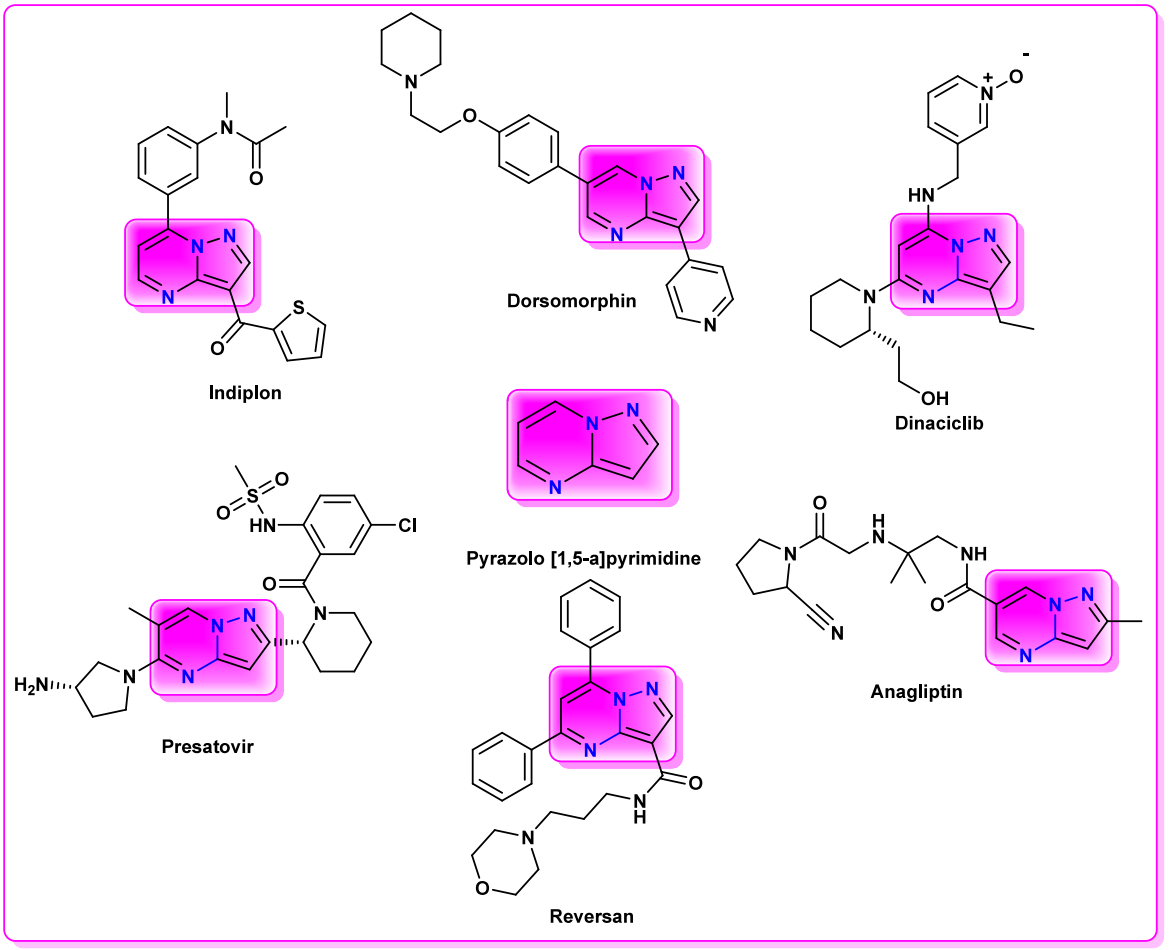

Figure 2. Representative examples of marketed drugs bearing a pyrazolo[1,5-*a*]pyrimidine scaffold are highlighted in purple with various biological activities.

uridine diphospho-*N*-acetylglucosamine (UNAG) to receive enolpyruvate from phosphoenolpyruvate (PEP) by releasing inorganic phosphate. MurA is a crucial enzyme since it lacks a mammalian counterpart; besides, among both bacterial species, it is well-maintained. Thus, MurA is a prime candidate as an antibiotic discovery target due to its vital function in the synthesis of microbial cell walls and being absent in mammalian cells. Fosfomycin (I) is the only antibiotic used in clinics targeting MurA.[5] A popular antibacterial medication called fosfomycin (**I**) is a natural substance that specifically

https://doi.org/10.1021/acsomega.4c10286
ACS Omega 2025, 10, 4044−4056

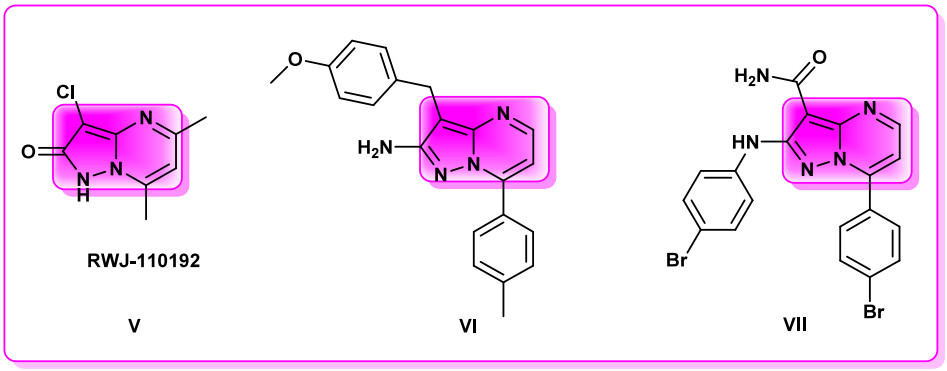

Figure 3. Structural representation of pyrazolo[1,5-*a*]pyrimidines as inhibitors of Mur enzymes.

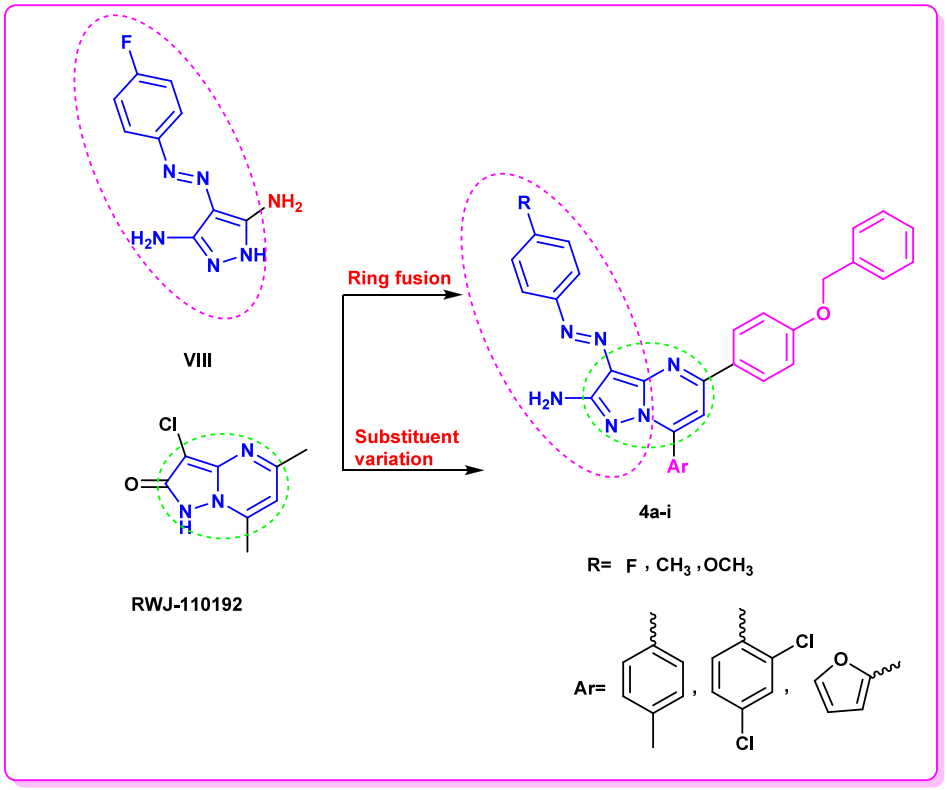

Figure 4. Design of new target compounds.

inhibits MurA enzyme.[6,7] Fosfomycin resistance developed as a result of different reasons, including alteration of the MurA active site or upregulation of MurA. Consequently, to combat this resistance, differently constructed MurA blockers with distinctive modes of activity must be developed. In prior literature reviews,[8,9] a diversity of chemically varied MurA inhibitors have been comprehensively described. Selections of inhibitors that have been recently discovered are illustrated in Figure 1. They exhibited micromolar inhibitory potencies against MurA and demonstrated antimicrobial activity against multiple bacterial strains. Compound **II**, which revealed considerable efficacy as evidenced by its IC_{50} value (half-maximal inhibitory concentration) of 1 μM, is recognized as one of the unique *Escherichia coli* MurA inhibitors originated by structure-based computational screening.[10] Moreover, **III** was shown to be an effective *E. coli* MurA inhibitor, having IC_{50} = 3.1 μM, according to the outcomes of a large-scale screening process of Novartis chemical collection.[3] Interestingly, **IV** bearing a benzyloxyphenyl moiety displayed promising inhibitory influence against MurA, with an IC_{50} of 8 μM.[7]

The pyrazolo[1,5-*a*]pyrimidine structural pattern is a planar nitrogen-containing heterocyclic framework comprising both pyrazole and pyrimidine scaffolds. The usage of such a fused pyrazole system offers significant benefits in the exploration of pharmaceutical compounds with considerable impact in the domain of medicinal chemistry. The remarkable synthetic flexibility of pyrazolo[1,5-*a*]pyrimidines has recently garnered considerable interest owing to their beneficial properties, which enable structural modifications at any position.[11,12] Different reported activities were recorded for such a scaffold, indicating its great importance. It has demonstrated significant therapeutic potential as anticancer comprising several kinase inhibitors,[13−16] antiviral (hepatetitis C and HIV),[17,18] COX-2 inhibitors,[19,20] antimicrobial,[21−23] and anxiolytic.[24,25] Furthermore, the biocompatibility and lower toxicity levels of

https://doi.org/10.1021/acsomega.4c10286
ACS Omega 2025, 10, 4044−4056

Scheme 1[a]

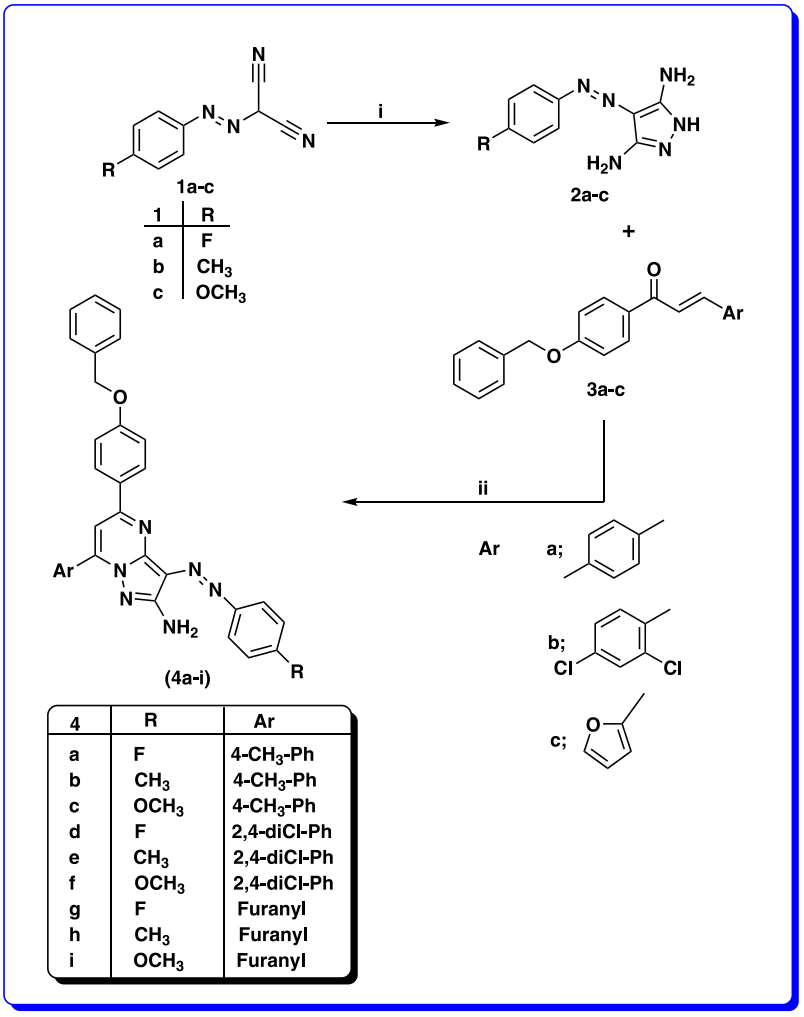

[a]Reagents and conditions: (i) $NH_2NH_2{\cdot}H_2O$; EtOH, reflux, 4 h. (ii) EtOH/Pip., reflux, 5 h.

pyrazolo[1,5-*a*]pyrimidines have led them to be approved as commercialized drugs, for instance, Indiplon; sedative hypnotic, Dorsomorphin; selective inhibitor of bone morphogenetic protein (BMP) signaling, Reversan; selective inhibitor of P-glycoprotein (P-gp) and multidrug resistance-associated protein 1 (MRP1), Presatovir; antiviral, Anagliptin; antidiabetic,[11] and Dinaciclib; cyclin-dependent kinases (CDKs) inhibitor[26], as shown in Figure 2.

Interestingly, the pyrazolopyrimidine (RWJ-110192) **V** was reported as one of the MurA inhibitors that differs chemically from fosfomycin and was able to exhibit broad-spectrum activity when it binds noncovalently to MurA at or near the fosfomycin binding site.[6] Recently, different pyrazolo[1,5-*a*]pyrimidines were described as active antibacterial hits. Novel pyrazolo[1,5-*a*]pyrimidin-2-amines connected to substituted phenyl rings demonstrated a broad range of antibacterial efficacy; especially, compound **VI** recorded a marked antibacterial effect with MIC/MBC = 2.8/5.6 μM.[27−29] Compound **VII** displayed high potency against both species; besides, it is thought to interrupt the peptidoglycan pathway via inhibiting MurC as another member of Mur family[30] (Figure 3).

1.1. Rational Molecular Design. Building on the antimicrobial activity observed with pyrazolopyrimidine (RWJ-110192) **V**, particularly its inhibition against the MurA enzyme, as well as the potent antimicrobial effects of the arylazopyrazole derivative **VIII**, which exhibited an MIC of 12.5 μg/mL against a wide range of microorganisms,[31] our design strategy (Figure 4) focuses on conserving the arylazopyrazole core and the 2 amino group, besides undergoing a ring fusion strategy on the pyrazole backbone producing the pyrazolo[1,5-*a*]pyrimidine moiety. Moreover, substitution on the pyrimidine ring at position 5 with a benzyloxy phenyl moiety is preserved in all derivatives. Employing the substituent variation strategy, substitution at position 7 was carried out with different aromatic or heteroaromatic derivatives to discover the influence of various substituents on activity. "Based on the aforementioned, novel compounds of substituted arylazo pyrazolo[1,5-*a*]pyrimidines were synthesized to investigate their antibacterial properties."

To measure the antimicrobial efficacy of the new hits, all derivatives were tested to determine their minimum inhibitory concentration (MIC), minimum bactericidal concentration (MBC), and minimum fungicidal concentration (MFC) in comparison to those of the market drugs. Additionally, an *in vitro* MurA enzyme inhibitory experiment was done. Moreover, the impact of the most promising compound **4c** on the development of biofilms and the activity of hemolysis by *E. coli*

https://doi.org/10.1021/acsomega.4c10286
ACS Omega 2025, 10, 4044−4056

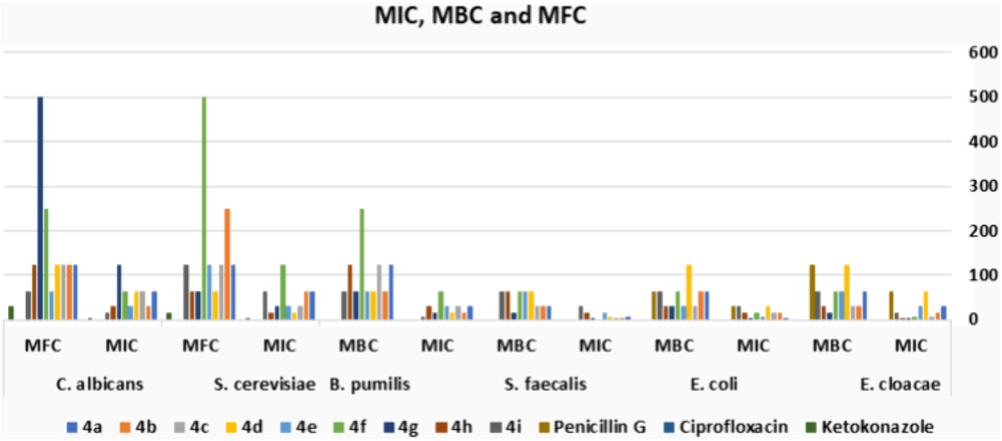

Figure 5. MIC, MBC, and MFC of the tested compounds.

and *Streptococcus faecalis* microorganisms was assessed to determine its effectiveness in preventing biofilm formation and reducing hemolysis. The binding score and interactions of compound **4c** were identified by molecular docking conducted inside the MurA binding site.

2. RESULTS AND DISCUSSION

2.1. Chemistry. Scheme 1 displays the production of nine new targeted compounds. Allowing the described technique,[32] the starting compounds, arylazo derivatives **1a−1c**, were made by diazotizing the relevant arylamines and then condensing with malononitrile. After cyclizing **1a−1c** using hydrazine hydrate and ethanol under reflux for 4 h, the intermediate compounds, 4-(arylazo)-1*H*-pyrazole-3,5-diamines **2a−2c**, were generated. The products were obtained in satisfactory yields.[33] The target compounds, 5,7-diaryl pyrazolo[1,5-*a*]pyrimidines, **4a−4i**, were prepared by cyclocondensation of substituted chalcones **3a−3c** with 4-(arylazo)-1*H*-pyrazole-3,5-diamines **2a−2c**, in ethanol/piperidine.[34] The chemical structures of the prepared molecules were verified. The ^{1}H NMR spectra for compounds **4a−4i** shared a common feature, which is a singlet at the range of δ (5.21−5.23) ppm representing OCH_2 protons, in addition to the appearance of a pyrimidine proton and an increase in the number of aromatic protons. The ^{13}C NMR spectra for all derivatives revealed the existence of a peak at the δ (69.43−69.53) ppm range referred to as the OCH_2 carbon. Taking **4a** as a representative example of this series, the spectrum of IR displayed the incidence of the NH_2 group at 3430 and 3312 cm^{-1}, whereas the ^{1}H NMR spectrum displayed two singlets at δ 2.44 and 5.23 ppm corresponding to the CH_3 and OCH_2 protons, respectively. Furthermore, a new singlet at δ 7.74 ppm appeared, representing the pyrimidine proton. The other aromatic protons appeared as multiples at δ 7.19−7.51 and 7.89−7.93 ppm for 15 protons and doublet of doublet for 4 protons at δ 7.09−8.36 ppm. In the spectrum of ^{13}C NMR of **4a**, CH_3 and OCH_2 carbons were located at peaks 21.10 and 69.44 ppm, respectively, while the aromatic carbons in direct contact with the oxygen and fluorine atoms were found downfield at 159.09 and 160.50 ppm. Its mass spectrum established the structure with a molecular ion peak [M^{+}, 45.74%] at m/z 528.

2.2. Biological Studies. The microbroth dilution assay, which is used to calculate MICs in accordance with CLSI reference standards, was employed to measure the antibacterial activity of the produced molecues. Herein, four different types of bacteria, namely, *Bacillus pumilis* (MTCC- 2296), *S. faecalis* (MTCC- 0459), *E. coli* (ATCC- 25955), and *Enterobacter cloacae* (ATCC- 23355), and two fungus strains, namely, *Saccharomyces cerevisiae* (ATCC-9763) and *Candida albicans* (ATCC-10231), were selected to evaluate antimicrobial properties. To compare the compound activity, penicillin G, ciprofloxacin, and ketoconazole were utilized as standards. The summarized antibacterial and antifungal results by performing MIC, MBC, and MFC assays were depicted in Tables S1 and S2 (Supporting Information). The IZ and MIC/MBC assessments were done twice, and the results in the manuscript are the mean of them.

2.2.1. MIC, MBC, and MFC. Results for MIC, MBC, and MFC were considered for further investigation. The relations between MBC/MIC and MFC/MIC were measured. The results obtained are illustrated in Tables S1 and S2 in the Supporting Information.

2.2.1.1. MIC and MBC. In the assessment of Gram-positive bacteria, all analogues exhibited a significantly elevated inhibitory activity relative to the reference antibiotic penicillin G. Moreover, derivatives **4g** and **4h** containing a furan moiety demonstrated significant efficacy against *B. pumilis*, exhibiting 16 times greater potency than the conventional penicillin G (MIC; 3.91 vs 62.5 μg/mL). Compounds **4c** and **4f** showed an 8-fold increase in activity compared to the reference, penicillin G, against *B. pumilis*, with MIC = 7.81 μg/mL. Additionally, derivatives **4b** and **4i** exhibited a 4-fold greater action than penicillin G, having MIC = 15.6 μg/mL. Compounds **4a**, **4e**, and **4g** exhibited antibacterial potencies that were 8, 4, and 16 times greater, respectively, having MIC = 3.91, 7.81, and 1.95 μg/mL, respectively. On other hand, compounds **4b**, **4c**, **4f**, and **4h** showed antibacterial activity twice as strong as penicillin G, the reference compound (MIC; 15.6 vs 31.5 μg/mL), against *S. faecalis*.

The demonstration of antibacterial activity in compounds deemed bactericidal is contingent upon the MBC not exceeding four times the MIC value. Concerning the MBC results, the majority of the evaluated compounds exhibited significant MBC/MIC ratios of ≤4, signifying their bactericidal properties. Compounds **4a−4e**, **4g**, and **4i** demonstrated enhanced efficacy against *B. pumilis*, with MBC values ranging from 15.6 to 125 μM (MBC/MIC ratios: 2 and 4). Furthermore, compounds **4b−4f**, **4h**, and **4i** showed substantial bactericidal activity against *S. faecalis*, with MBC values between 31.3 and 125 μM (MBC/MIC ratios: 2 and 4).

https://doi.org/10.1021/acsomega.4c10286
ACS Omega 2025, 10, 4044−4056

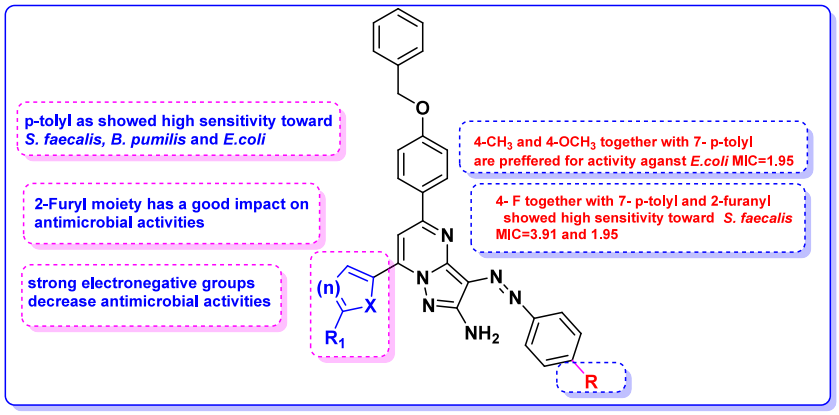

Figure 6. SAR of the antimicrobial activity of **4a−4i**.

Concerning Gram-negative strains, the new compounds displayed a slight to reasonable efficacy. Among the synthesized derivatives, compounds **4b** and **4c** demonstrated exceptionally potent anti G-ve bacteria activity against *E. coli* with MIC = 1.95 μg/mL. Also, **4i** showed a noteworthy effect against *E. cloacae*, having an MIC value = 7.81 μg/mL.

About the minimum bactericidal concentrations (MBC), compounds **4a** and **4e−4i** demonstrated marked bactericidal action on *E. coli* with MBC/MIC ratios 2 and 4. The new derivatives indicated a strong bactericidal profile against *E. cloacae* with MBC/MIC ratios 2 and 4 except compound **4i** that has an MBC/MIC ratio equal to 8.

2.2.1.2. MIC and MFC. Measuring the effect on fungi strains, the investigated hits showed modest to moderate action on the tested fungus strains (Table S2 and Figure 5). Compounds **4d** and **4h** demonstrated high inhibitory efficacy against *S. cerevisiae,* with MIC = 15.6 μg/mL. Also, **4i** exhibited good efficacy on *C. albicans* with MIC = 15.6 μg/mL. With respect to MFC, the newly synthesized compounds that were evaluated had a notable MFC/MIC of roughly ≤4, signifying their fungicidal effect against *S. cerevisiae* and *C. albicans* (MFC/MIC ratios: 2 and 4).

2.2.2. Structure−Activity Relationship (SAR). The presented antimicrobial findings indicated that the antimicrobial profile was significantly impacted by the type of 7-aryl moiety. Once the aryl group is *p*-tolyl as in derivatives **4a−4c**, it showed sensitivity toward *S. faecalis*, *B. pumilis*, and *E. coli*. In addition, the analogues **4b** and **4c** bearing 4-CH_3 and 4-OCH_3 on the phenyl-azo moiety presented the best activity against *E. coli*. The enhanced activity of the analogues **4b** and **4c**, bearing 4-CH_3 and 4-OCH_3 groups on the phenyl-azo moiety, against *E. coli* can be attributed to several factors: Electronic effects: The presence of electron-donating groups such as methyl (CH_3) and methoxy (OCH_3) increases electron density on the phenyl ring. This can enhance the compound's ability to interact with bacterial targets, potentially improving binding affinity and disrupting bacterial processes. Hydrophobic interactions: Both the 4-CH_3 and 4-OCH_3 groups contribute to the hydrophobic character of the molecule. This may facilitate better membrane penetration or interaction with lipid components in bacterial cells, enhancing antibacterial efficacy. Steric factors, these substituents may also influence the steric arrangement of the molecule, optimizing it for interaction with specific bacterial enzyme.

Alternatively, the replacement of the substituted phenyl ring by the 2,4-diCl-ph ring on carbon 7 of the pyrazolo[1,5-*a*]pyrimidine core (while preserving the same substituent on the phenyl group at position 3), as in compounds **4d−4f**, revealed lower antibacterial activity than the previous derivatives. This means that the strong electron-withdrawing outcome of the 2,4-diCl-ph ring in **4d−4f** reported low efficacy. The strong electron-withdrawing nature of the 2,4-diCl-phenyl ring reduces electron density on the molecule, which may impair its ability to interact with certain bacterial targets. However, compound **4d** displayed better fungicidal activity against *S. cerevisiae*.

It is noteworthy that, when the aryl moiety on carbon 7 is furan as in compounds **4g−4i**, it demonstrated remarkably strong antibacterial potential against *S. faecalis* and *B. pumilis* as in **4g**, **4h**, and **4i**. Moreover, compound **4h** showed good activity against *S. cerevisiae*. At the same time, **4i** displayed the highest inhibitory efficacy toward *C. albicans*. The strong antibacterial potential of compounds with a furan moiety on carbon 7 may be due to several reasons such as its unique electronic structure facilitating strong interactions with bacterial targets, the hydrophobic nature of furan that allows for efficient membrane penetration, leading to increased accumulation of the compound within bacterial cells, and its structural flexibility that enables optimal accommodation in active sites, enhancing binding affinity to critical bacterial enzymes (Figure 6).

2.2.3. MurA Inhibitory Effect. Using fosfomycin as a standard medication, the MurA inhibition experiment was conducted to determine the mechanism of action of **4c**, which demonstrated marked efficacy on the tested microorganisms in accordance with the antibacterial and MIC values. The results were conveyed by IC_{50} (μg/mL) and are displayed in Figure 7. The pyrazolo[1,5-*a*]pyrimidine **4c** demonstrated a w80 effect on the MurA enzyme with IC_{50} = 3.27 ± 0.2 μg/mL compared with fosfomycin having an IC_{50} of 9.63 ± 0.58 μg/mL.

Moreover, the *in vitro* toxic effect of compound **4c** on normal human cells (WI38) was evaluated to determine its safety. The results demonstrated that compound **4c** was safe as it has a high IC_{50} value (IC_{50} = 47.0 ± 2.86 μM).

2.2.4. Antibiofilm Activity. It is widely recognized that before bacteria produce virulence factors and interfere with host defense mechanisms in infectious diseases, they must achieve a particular cell density. Pathogenic bacteria have evolved an extraordinary mechanism known as "biofilm formation"[35] to withstand the deadly blows of antibiotics or the host immune system, oxidative stress, and malnutrition. A biofilm is a collection of bacteria that stick to a biotic or abiotic

https://doi.org/10.1021/acsomega.4c10286
ACS Omega 2025, 10, 4044−4056

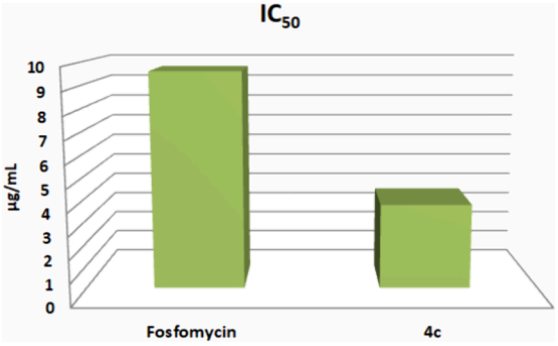

Figure 7. IC_{50} of fosfomycin and compound **4c** against MurA.

surface within an extracellular polymeric substance (EPS) matrix.[36,37] Consequently, there is a pressing need for newly developed molecules or combinations with current drugs that can either inhibit or degrade the biofilm framework. Herein, we tested compound **4c** against *E. coli* and *S. faecalis* microorganisms as examples of G-ve and G+ve, respectively, as revealed in Figures 8 and 9. The results indicated that

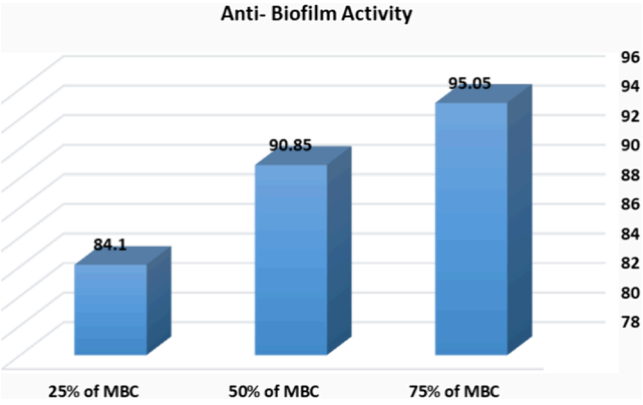

Figure 8. Antibiofilm activity of compound **4c** on *E. coli*.

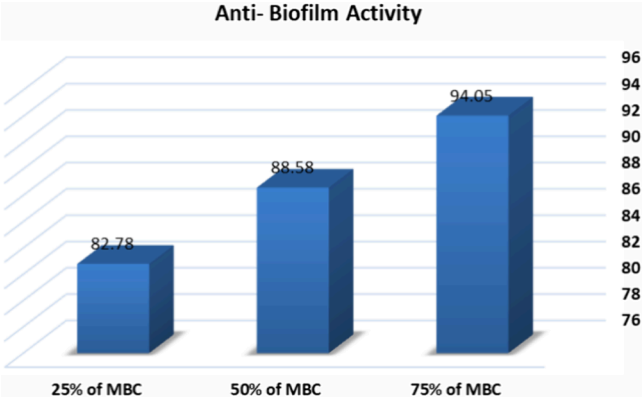

Figure 9. Antibiofilm activity of compound **4c** on *S. faecalis*.

compound **4c** significantly inhibited the biofilm formation of *E. coli* by 95.05% and *S. faecalis* by 94.05% at 75% MBC. In other words, the antibiofilm activity increases as the percentage of MBC increases. Tables S3 and &S4 are available in the Supporting Information.

2.2.5. Hemolytic Activity Assay. The term hemolysis describes the disintegration of red blood cells or erythrocytes (RBCs). Erythrocytes are destroyed as a result, releasing hemoglobin from red blood cells into the plasma of the blood.[38] The hemolytic assay was performed on both *E. coli* and *S. faecalis* bacteria to assess the capacity of compound **4c** to hinder the hemolytic activity. The obtained results indicated an interesting relationship between the minimum inhibitory concentration (MIC) of compound **4c** and its hemolytic activity on red blood cells (RBCs). Specifically, the observation that higher percentages of MIC lead to lower hemolysis suggests a favorable safety profile for compound **4c** as a potential antibacterial agent. Compound **4c** significantly showed hemolysis of *E. coli* by 7.1% and *S. faecalis* by 3.3% at 75%MBC, compared with the control (100% hemolysis), as shown in Figures 10 and 11.

2.3. Docking Study. The MurA enzyme participates in the synthesis of the bacterial cell wall, namely, in peptidoglycan biosynthesis, which is an essential element of the cellular structure known as the cell wall. Peptidoglycan has a significant function in maintaining the structure and integrity of bacterial cells. It is also involved in cell development and division. When the synthesis of PG is disrupted, it leads to cell lysis, which prevents bacterial survival.[39−43]

MurA's crystal structure comprises two domains, where the active site is positioned between them.[44] This section has a multitude of residues with side chains that are highly functionalized: Asn23, Asp49, Arg91, Arg120, Asp231, Asp305, Arg331, Arg371, Arg397 Gly164, Lys22, Phe328, Ser162, and Val163.[31] MurA's crystal structure, having the accession code 3kr6, is now accessible through the Protein Data Bank. Docking experiments were achieved via AutoDock Vina, a software program that specifically requires both ligands and receptors being in pdbqt format.[45] After redocking the cocrystallized ligand onto the complex enzyme, the computed root-mean-square deviation (RMSD) for both cocrystallized and docked ligands was 0.173 Å. This confirms the validity of the docking procedure. Results were visually depicted by the Discovery Studio 4.5 visualizer.[46] Experiments were performed to dock fosfomycin and compound **4c** into the active binding site of MurA. Table 1 shows the docking interactions of fosfomycin and **4c** having significant activity as a MurA enzyme inhibitor.

The positioning of fosfomycin and **4c** in the binding region of the enzyme was achieved by using a docking approach. Compounds under investigation achieved docking scores = −7.0 and −11.9 kcal/mol, respectively. Fosfomycin formed conventional hydrogen bonding interactions with Arg120, Cys115, and Lys22 in a characteristic manner. In addition, with Arg120, it built a salt bridge and exhibited attractive charge connections by Lys22, Asp49, Arg120, and Arg397, as presented in Figure 12. The examination of the anticipated binding mode of compound **4c** revealed that it is encompassed by the essential amino acids located within the binding site. The benzyloxy moiety's terminal phenyl ring formed a pi-cation connection with Arg397, a pi-donor hydrogen bond with Cys115, and a pi-cation;pi-donor hydrogen bond interaction with Arg91. Arg120 and Asp305 contributed through pi-cation and pi-anion interactions, respectively, with the linked phenyl ring to the oxygen atom of the benzyloxy group. Additionally, the pyrazolo[1,5-*a*]pyrimidine scaffold formed a pi-sigma interaction with Val163 and Val327. Furthermore, the terminal NH_2 is shared by a conventional hydrogen bond with Val161. The phenyl ring connected to the N=N bridge formed a pi-anion connection with Arg91, whereas the *para*-methyl phenyl ring linked with His299 and

https://doi.org/10.1021/acsomega.4c10286
ACS Omega 2025, 10, 4044−4056

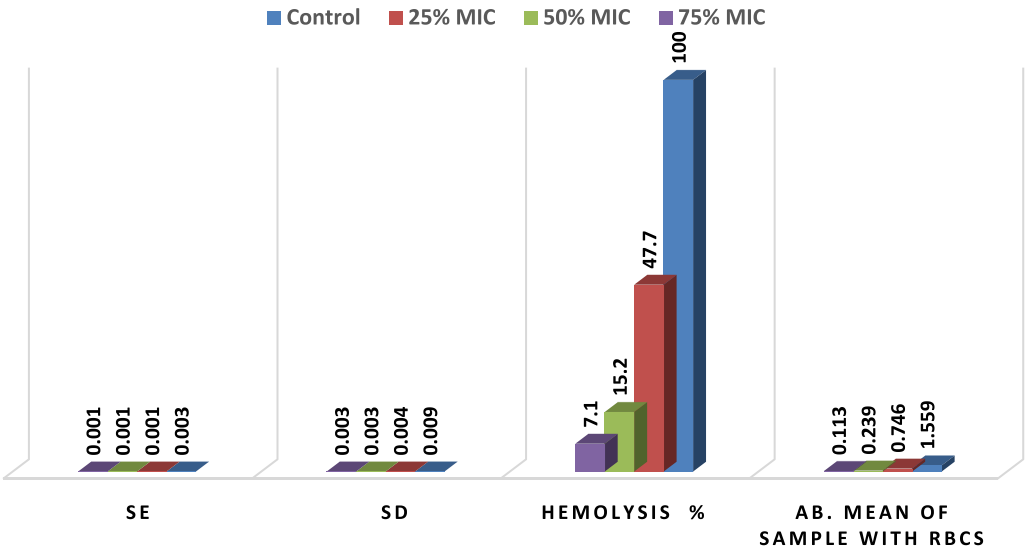

Figure 10. Antihemolytic activity of compound **4c** on *E. coli*.

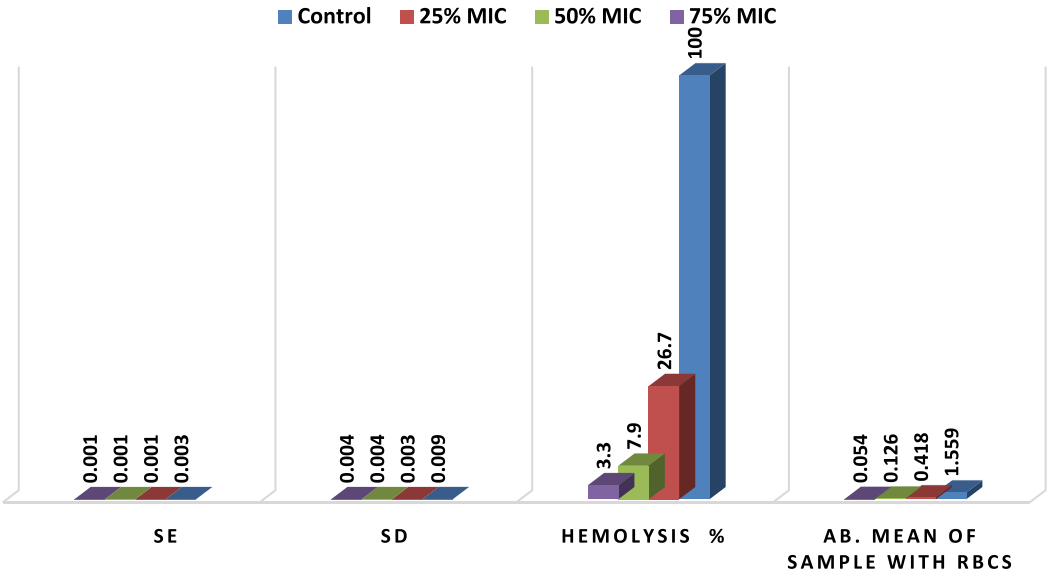

Figure 11. Antihemolytic activity of compound **4c** on *S. faecalis*.

Pro303 by a pi-alkyl interaction and Glu188 by a pi-anion interaction (Figure 13).

3. CONCLUSIONS

This study examined the antibacterial effectiveness of new pyrazolo[1,5-*a*]pyrimidine hits. Each of the newly produced derivatives had a notably strong ability to inhibit the growth of the selected microbes, as compared to the reference drugs. Compound **4c** exhibited significant antibacterial activity and was chosen for further evaluation. Its efficacy against both G +ve and G-ve bacteria highlights its broad-spectrum potential. It displayed strong effectiveness as a MurA inhibitor, with IC_{50} = 3.77 ± 0.2 μg/mL compared to fosfomycin. In addition, **4c** demonstrated high levels of antibiofilm and antihemolytic activities, suggesting it may effectively combat bacterial infections associated with biofilm formation, which is a common challenge in clinical settings. Compound **4c** not only demonstrates the highest antibacterial activity and potent MurA inhibition but also effectively binds to the MurA enzyme. This strong binding affinity likely contributes to its remarkable efficacy against both G+ve and G-ve bacteria. These combined attributes make compound **4c** a promising agent for further investigation in the fight against bacterial infections.

4. EXPERIMENTAL SECTION

4.1. Chemistry. *4.1.1. Synthesis.* For the instruments and materials, see the Supporting Information. 4-(Arylazo)-3,5-diamino-1*H*-pyrazoles (**2a**−**2c**)[47,48] and 1-(4-(benzyloxy)-phenyl)-3-phenylprop-2-enone derivatives (**3a**−**3c**)[49,50] were prepared using the previously described processes.

*4.1.2. General Method for the Synthesis of Compounds **4a**−**4i**.* A solution comprising equal amounts (0.002 mol) of **2a**, **2b**, or **2c** and the corresponding substituted chalcone **3a**−**3c** (0.002 mol) was refluxed for 5 h in 20 mL of 95% ethanol, with the addition of three drops of piperidine as a catalyst. The isolated crystals were subjected to filtration, desiccation, and subsequent recrystallization using ethanol as the solvent.

*4.1.2.1. 5-(4-(Benzyloxy)phenyl)-3-((4-fluorophenyl)-diazenyl)-7-(p-tolyl)pyrazolo[1,5-a]pyrimidin-2-amine (**4a**).*

https://doi.org/10.1021/acsomega.4c10286
ACS Omega 2025, 10, 4044−4056

Table 1. Docking Scores and Interactions of Fosfomycin and 4c

	distance	type of interaction	amino acid
fosfomycin	2.88104	salt bridge	A:ARG120:NH1
	4.89607	attractive charge	A:LYS22:NZ
	3.0598	attractive charge	A:LYS22:NZ
	5.24051	attractive charge	A:ARG120:NH1
	3.46236	attractive charge	A:ARG397:NH2
	3.18373	attractive charge	A:ARG397:NH2
	4.59343	attractive charge	A:ASP49:OD2
	2.85194	conventional hydrogen bond	A:LYS22:NZ
	2.94222	conventional hydrogen bond	A:CYS115:N
	3.29458	conventional hydrogen bond	A:CYS115:SG
	2.99011	conventional hydrogen bond	A:ARG120:NH2
	4.06942	alkyl	A:CYS115
4c	3.10664	conventional hydrogen bond	A:VAL161:O
	3.69318	carbon hydrogen bond	A:SER162:CA
	3.54658	pi-cation; pi-donor hydrogen bond	A:ARG91:NH2
	4.46341	pi-cation	A:ARG120:NH2
	4.16196	pi-cation	A:ARG397:NH1
	2.71826	pi-anion	A:GLU188:OE1
	3.49989	pi-anion	A:ASP305:OD2
	3.36674	pi-donor hydrogen bond	A:CYS115:SG
	3.47627	pi-sigma	A:VAL163:CG2
	3.29879	pi-sigma	A:VAL163:CG2
	3.93715	pi-sigma	A:VAL327:CG1
	3.85784	alkyl	A:PRO303
	5.09715	pi-alkyl	A:HIS299
	5.04981	pi-alkyl	A:PRO303
	4.92486	pi-alkyl	A:ARG91

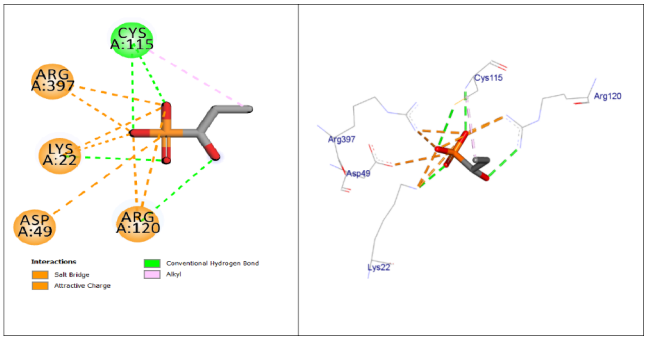

Figure 12. 2D and 3D images of fosfomycin in the MurA active binding site.

Yield: 50%; mp 153−155 °C; IR (KBr, cm^{-1}): 3430, 3312 (NH_2) 1599 (C=N); ^{1}H NMR (DMSO-d_6) (ppm): δ 2.44 (s, 3H, CH_3), 5.23 (s, 2H, OCH_2), 7.20−7.51 (m, 13H, OCH_2-C_6H_4-H_{2-6}+N=N-(4-F-C_6H_4-$H_{2,3,5,6}$+Ar_$H_{3,5}$) +NH_2), 7.74 (s, 1H, pyrimidine-H), 7.90−7.93(m, 2H, Ar-$H_{2,6}$+), 8.08 (d, 2H, Ph-$H_{3,5}$, AB sys, J = 8 Hz), 8.36 (d, 2H, Ph-$H_{2,6}$, AB sys, J = 8 Hz); ^{13}C NMR (400 MHz, DMSO-d_6) δ (ppm): 21.10 ($\underline{C}H_3$), 69.44($O\underline{C}H_2$), 104.95, 114.75, 115.12, 115.79 (d, ^{2}JCF, 22 Hz), 116.01, 122.85 (d, ^{3}JCF, 9 Hz), 122.94, 127.76, 127.83, 127.96, 128.48, 128.88, 129.04, 129.74, 136.74, 141.00, 145.51, 147.68, 149.85, 152.02, 156.09, 160.60 (d, ^{1}JCF, 252 Hz), 160.82, 162.25, 163.12; MS [m/z, %]: 528 [M^+, 22.80]; Anal. Calcd for $C_{32}H_{25}FN_6O$ (%): C, 72.71; H, 4.77; N, 15.90. Found: C, 72.72; H, 4.76; N, 15.91.

*4.1.2.2. 5-(4-(Benzyloxy)phenyl)-7-(p-tolyl)-3-(p-tolyldiazenyl)pyrazolo[1,5-a]pyrimidin-2-amine (**4b**).* Yield: 54%; mp 120−123 °C; IR (KBr, cm^{-1}): 3436, 3294, (NH_2); 1595 (C=N); ^{1}H NMR (DMSO-d_6): δ 2.38, 2.44 (2s, 6H, $2CH_3$), 5.23 (s, 2H, OCH_2), 7.20−7.51 (m, 11H, OCH_2-C_6H_4-H_{2-6}+N=N-(4-CH_3-C_6H_4-$H_{3,5}$)+Ar-$H_{3,5}$+NH_2), 7.68−7.77 (m, 5H, N=N-(4-CH_3-C_6H_4-$H_{2,6}$)+Ar-$H_{2,6}$+pyrimidine-H), 8.09 (d, 2H, Ph-$H_{3,5}$, AB sys, J = 8 Hz), 8.36 (d, 2H, Ph-$H_{2,6}$, AB sys, J = 8 Hz); ^{13}C NMR (400 MHz, DMSO-d_6) δ (ppm): 20.99 ($\underline{C}H_3$), 21.20 ($\underline{C}H_3$), 69.53 ($O\underline{C}H_2$), 104.85, 114.69, 115.24, 121.16, 127.87,127.92, 128.08, 128.60, 129.01, 129.13,129.19, 129.76, 129.80, 136.83, 138.17, 141.13, 145.58, 147.62, 151.14, 152.15, 156.13, 160.65; MS [m/z, %]: 524 [M^+, 32.63%]; Anal. Calcd for $C_{33}H_{28}N_6O$ (%): C, 75.55; H, 5.38; N, 16.02. Found: C, 75.53; H, 5.36; N, 16.01.

*4.1.2.3. 5-(4-(Benzyloxy)phenyl)-3-((4-methoxyphenyl)-diazenyl)-7-(p-tolyl)pyrazolo[1,5-a]pyrimidin-2-amine (**4c**).* Yield: 55%; mp 172−175 °C; IR (KBr, cm^{-1}): 3403, 3293 (NH_2), 1596 (C=N); ^{1}H NMR (DMSO-d_6): δ 2.43 (s, 3H, CH_3), 3.83 (s, 3H, OCH_3), 5.22 (s, 2H, OCH_2), 7.06 (d, 2H, Ar-$H_{3,5}$ AB sys, J = 8 Hz), 7.16−7.20 (m, 3H, OCH_2-C_6H_4-H_4+N=N-(4-OCH_3-C_6H_4-$H_{3,5}$), 7.35−7.51 (m, 8H, N=N-(4-OCH_3-C_6H_4-$H_{2,6}$)+OCH_2-C_6H_4-$H_{2,3,5,6}$+NH_2), 7.68 (s, 1H, pyrimidine-H), 7.83 (d, 2H, Ar-$H_{2,6}$ AB sys, J = 8 Hz), 8.08 (d, 2H, Ph-$H_{3,5}$ AB sys, J = 8 Hz), 8.34 (d, 2H, Ph-$H_{2,6}$ AB sys, J = 8 Hz); ^{13}C NMR (400 MHz, DMSO-d_6) δ (ppm): 21.11 ($\underline{C}H_3$), 55.41 ($O\underline{C}H_3$), 69.43 ($O\underline{C}H_2$), 104.45, 114.31, 115.08, 122.58, 127.82, 127.85, 127.96, 128.48, 128.87, 128.97, 129.17, 129.69, 136.75, 140.93, 145.33, 147.23, 147.32, 152.04, 155.79, 159.67, 160.51; MS [m/z, %]: 542 [M+2, 34.74%]; Anal. Calcd for $C_{33}H_{28}N_6O_2$ (%): C, 73.32; H, 5.22; N, 15.55. Found: C, 72.99; H, 5.20; N, 15.49.

*4.1.2.4. 5-(4-(Benzyloxy)phenyl)-7-(2,4-dichlorophenyl)-3-((4-fluorophenyl)diazenyl)pyrazolo[1,5-a]pyrimidin-2-amine (**4d**).* Yield: 53%; mp 113−115 °C; IR (KBr, cm^{-1}): 3282, 3248 (NH_2), 1591 (C=N); ^{1}H NMR (DMSO-d_6): δ 5.22 (s, 2H, OCH_2), 7.19−7.50 (m, 11H, Ph-$H_{3,5}$+N=N(4F-C_6H_4-$H_{2,3,5,6}$)+OCH_2-C_6H_4-$H_{3,4,5}$+NH_2), 7.68−7.94 (m, 6H, OCH_2-C_6H_4-$H_{2,6}$+Ar-$H_{3,5,6}$+pyrimidine-H), 8.33 (d, 2H, Ph-$H_{2,6}$); ^{13}C NMR (400 MHz, DMSO-d_6) δ (ppm): 69.46 ($O\underline{C}H_2$), 106.40, 114.89, 115.79 (d, ^{2}JCF, 23 Hz), 116.02, 122.95 (d, ^{3}JCF, 8 Hz), 123.03, 127.58, 127.82, 128.46, 129.04, 129.17, 129.44, 129.65, 130.20, 131.12, 132.88, 133.19, 135.92, 135.67, 142.64, 146.75, 149.81, 152.31, 155.94, 160.77 (d, ^{1}JCF, 246 Hz), 163.23; MS [m/z, %]: 583 [M^+, 49.80%], 585 [$(M+2)^+$, 16.64%]; Anal. Calcd for $C_{31}H_{21}Cl_2FN_6O$ (%): C, 63.82; H, 3.63; N, 14.40. Found: C, 63.81; H, 3.64; N, 14.39.

*4.1.2.5. 5-(4-(Benzyloxy)phenyl)-7-(2,4-dichlorophenyl)-3-(p-tolyldiazenyl)pyrazolo[1,5-a]pyrimidin-2-amine (**4e**).* Yield: 49%; mp 163−165 °C; IR (KBr, cm^{-1}): 3354, 3277 (NH_2), 1597 (C=N); ^{1}H NMR (DMSO-d_6): δ 2.34 (s, 3H, CH_3), 5.22 (s, 2H, OCH_2), 7.07−7.53 (m, 13H, OCH_2-C_6H_4-H_{2-6}+N=N-(4CH_3-C_6H_4-$H_{3,5}$)+Ph-$H_{3,5}$+Ar-$H_{2,5}$+NH_2), 7.71−7.81 (m, 4H+N=N-(4CH_3-C_6H_4-$H_{2,6}$)+Ar-H_6+pyrimidine-H), 8.32 (d, 2H, Ph-$H_{2,6}$); ^{13}C NMR (400 MHz, DMSO-d_6) δ (ppm): 20.90 ($\underline{C}H_3$), 69.46 ($O\underline{C}H_2$), 106.20, 114.60, 114.81, 121.04, 127.59, 127.82, 127.96, 128.76, 129.03, 129.36, 129.70, 132.89, 133.80, 135.89, 136.68, 136.89, 138.20, 142.59, 146.60, 151.03, 152.35, 155.81,158.91, 160.74; MS [m/z, %]: 579 [M^+, 32.81%], 581 [$(M+2)^+$, 12.64%];

https://doi.org/10.1021/acsomega.4c10286
ACS Omega 2025, 10, 4044−4056

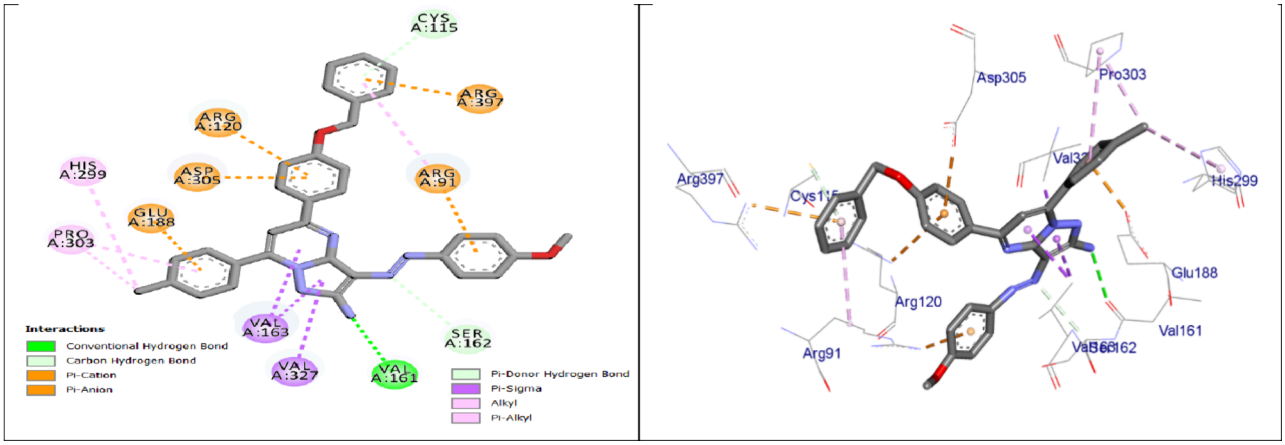

Figure 13. 2D and 3D images of **4c** in the MurA active binding site.

Anal. Calcd for $C_{32}H_{24}Cl_2N_6O$ (%): C, 66.33; H, 4.17; N, 14.50. Found: C, 66.35; H, 4.19; N, 14.52.

*4.1.2.6. 5-(4-(Benzyloxy)phenyl)-7-(2,4-dichlorophenyl)-3-((4-methoxyphenyl)diazenyl)pyrazolo[1,5-a]pyrimidin-2-amine (**4f**).* Yield: 56%; mp 113−115 °C; IR (KBr, cm^{-1}): 3358, 3248 (NH_2), 1595 (C=N); ^{1}H NMR (DMSO-d_6): δ 3.83 (s, 3H, OCH_3), 5.22 (s, 2H, OCH_2), 7.07−7.92 (m, 17H, Ph-$H_{3,5}$+OCH_2-C_6H_4-H_{2-6}+N=N-(4-OCH_3-C_6H_4-$H_{2,3,5,6}$)+pyrimidine-H+Ar-$H_{3,5,6}$+NH_2), 8.33 (d, 2H, Ph-$H_{2,6}$); ^{13}C NMR (400 MHz, DMSO-d_6) δ (ppm): 55.42 ($O\underline{C}H_3$), 69.46 ($O\underline{C}H_2$), 105.91, 114.32, 115.21, 122.66, 127.59, 127.74, 127.82, 127.96, 128.47, 128.83, 128.99, 129.17, 129.75, 132.88, 133.81, 135.86, 136.69, 142.51, 146.37, 147.19, 152.33, 155.62, 159.79, 160.69; MS [*m*/*z*, %]: 595 [M^+, 43.71%], 597 [$(M+2)^+$, 29.10%]; Anal. Calcd For $C_{32}H_{24}Cl_2N_6O_2$ (%): C, 64.54; H, 4.06; N, 14.11. Found: C, 64.50; H, 4.10; N, 14.13.

*4.1.2.7. 5-(4-(Benzyloxy)phenyl)-3-((4-fluorophenyl)-diazenyl)-7-(furan-2-yl)pyrazolo[1,5-a]pyrimidin-2-amine (**4g**).* Yield: 56%; mp 182−185 °C; IR (KBr, cm^{-1}): 3416, 3355 (NH_2), 1592 (C=N); ^{1}H NMR (DMSO-d_6): δ 5.22 (s, 2H, OCH_2), 6.95 (t, 1H, OCH_2-C_6H_4-H_4), 7.18−7.52 (m, 10H, N=N-(F-C_6H_4-$H_{2,3,5,6}$)+Ph_$H_{3,5}$+OCH_2-C_6H_4-$H_{3,5}$+NH_2), 7.69−7.73 (m, 2H+furan-$H_{3,5}$), 7.89−7.94 (m, 3H, pyrimidine-H+OCH_2-C_6H_4-$H_{2,6}$), 8.19 (t, 1H, furan-H_4), 8.30 (d, 2H, Ph-$H_{2,6}$); ^{13}C NMR (400 MHz, DMSO-d_6) δ (ppm): 69.44 ($O\underline{C}H_2$), 99.44, 114.4, 115.18, 115.32,115.54 (d, ^{2}JCF, 23 Hz), 116.03, 121.93 (d, ^{3}JCF, 8 Hz), 122.01, 122.99, 127.81, 127.96, 128.48, 128.84, 136.72, 143.24, 147.27, 147.40, 149.83, 150.32, 152.20,155.29, 159.66, 160.56 (d, ^{1}JCF, 276 Hz), 163.32; MS [*m*/*z*, %]: 504 [M^+, 37.91]; Anal. Calcd for $C_{29}H_{21}FN_6O_2$ (%): C, 69.04; H, 4.20; N, 16.66. Found: C, 69.02; H, 4.23; N, 16.67.

*4.1.2.8. 5-(4-(Benzyloxy)phenyl)-7-(furan-2-yl)-3-(p-tolyldiazenyl)pyrazolo[1,5-a]pyrimidin-2-amine (**4h**).* Yield: 58%; mp 212−215 °C; IR (KBr, cm^{-1}): 3410, 3395 (br., NH2), 1598 (C=N); ^{1}H NMR (DMSO-d_6): δ 2.38 (s, 3H,CH_3), 5.24 (s, 2H, OCH_2), 6.95 (t, 1H, OCH_2-C_6H_4-H_4), 7.22−7.52 (m, 12H, OCH_2-C_6H_4-$H_{2,3,5,6}$+N=N-(4-CH_3-C_6H_4-$H_{2,3,5,6}$+furan-$H_{3,5}$+NH_2), 7.77 (d, 2H, Ph-$H_{3,5}$,*J* = 8 Hz), 7.89 (s, 1H, pyrimidine-H), 8.19 (t, 1H, furan-H_4), 8.31 (d, 2H, Ph-$H_{2,6}$, *J* = 8 Hz); ^{13}C NMR (400 MHz, DMSO-d_6) δ (ppm): 20.91 ($\underline{C}H_3$), 69.45 ($O\underline{C}H_2$), 99.28, 113.33, 114.27, 115.23, 119.86, 120.35, 121.11, 127.83, 127.97, 128.50, 128.85, 129.16, 129.66, 134.28, 136.75, 138.15, 143.29, 147.27, 151,03, 152.25, 155.20, 160.54; MS [*m*/*z*, %]: 500 [M^+, 17.26]; Anal. Calcd for $C_{30}H_{24}N_6O_2$ (%): C, 71.99; H, 4.83; N, 16.79. Found: C, 71.97; H, 4.82; N, 16.78.

*4.1.2.9. 5-(4-(Benzyloxy)phenyl)-7-(furan-2-yl)-3-((4-methoxyphenyl)diazenyl)pyrazolo[1,5-a]pyrimidin-2-amine (**4i**).* Yield: 60%; mp 202−205 °C; IR (KBr, cm^{-1}): 3309,3270 (NH_2), 1593 (C=N); ^{1}H NMR (DMSO-d_6): δ 3.84 (s, 3H, OCH_3), 5.23 (s, 2H, OCH_2), 6.95−7.51(m, 14H, OCH_2-C_6H_4-H_{2-6}+N=N-(4-OCH_3-C_6H_4-$H_{2,3,5,6}$)+furan-$H_{3,5}$+pyrimidine-H+NH_2), 7.84 (d, 2H, Ph-$H_{3,5}$, *J* = 8 Hz), 8.19 (t, 1H, furan-H_4), 8.30 (d, 2H, Ph-$H_{2,6}$, *J* = 8 Hz); ^{13}C NMR (400 MHz, DMSO-d_6) δ (ppm): 55.42 ($O\underline{C}H_3$), 69.44 ($O\underline{C}H_2$), 79.16, 99.01, 113.28, 113.97, 114.32, 115.18, 119,75, 122.62, 127.81, 127.96, 128.48, 128.79, 129.20, 134.18, 136.74, 143.32, 147.03, 147.18, 152.21, 154.99, 159.75, 160.49; MS [*m*/*z*, %]: 516 [M^+, 10.23]; Anal. Calcd for $C_{30}H_{24}N_6O_3$ (%): C, 69.76; H, 4.68; N, 16.27. Found: C, 69.77; H, 4.67; N, 16.28.

4.2. Biological Evaluations. *4.2.1. Minimal Inhibition Concentration.* To assess the efficacy of recently synthesized substances in preventing the growing of tested microbes, the MIC, MBC, and MFC assays were conducted using the technique described in the reference papers.[51−53] Please refer to the Supporting Information for more details.

4.2.2. MurA Enzyme Inhibition Assay. In the Supporting Information, the process is clearly described.

4.2.3. Microtiter Plate Assay for Biofilm Quantification. The impact of **4c** on production of biofilms was assessed using 96-well polystyrene flatbottom plates. Please see the Supporting Information for more details.[54]

4.2.4. Hemolysin Inhibition Assay. See the Supporting Information for more details.[55]

4.3. Docking Study. Docking investigation took place via Vina Autodock. Protein database (PDB ID: 3KR6) was used to obtain the crystal structures of MurA enzyme. The studied compounds and MurA were edited to a pdbqt format during the docking process with Vina Autodock. The M.G.L. procedures were then employed to measure and assess the grid box that encircled the binding site. Utilizing the Biovia Discovery Studio 2020 Visualizer, the docking outcomes were applied to generate 3D and 2D predicted poses for the examined compounds.

https://doi.org/10.1021/acsomega.4c10286
ACS Omega 2025, 10, 4044−4056

■ ASSOCIATED CONTENT

Supporting Information

The Supporting Information is available free of charge at https://pubs.acs.org/doi/10.1021/acsomega.4c10286.

Copy of ^{1}H NMR and ^{13}C NMR of all synthesized compounds as well as experimental methods of biological assays and dose−response curves, *in vitro* MIC, MBC, and MBC/MIC ratio of the tested compounds, and antibiofilm activity of compound **4c** (PDF)

■ AUTHOR INFORMATION

Corresponding Author

Marwa F. Harras − *Department of Pharmaceutical Medicinal Chemistry and Drug Design, Faculty of Pharmacy (Girls), Al-Azhar University, Cairo 11651, Egypt;* orcid.org/0000-0003-4723-6179; Email: marwaharras.pharmg@azhar.edu.eg, marwa_harras@yahoo.com

Authors

Omkulthom Al kamaly − *Department of Pharmaceutical Sciences, College of Pharmacy, Princess Nourah bint Abdulrahman University, Riyadh 11671, Saudi Arabia*

Amel S. Younes − *Department of Pharmaceutical Medicinal Chemistry and Drug Design, Faculty of Pharmacy (Girls), Al-Azhar University, Cairo 11651, Egypt*

Mona H. Ibrahim − *Department of Pharmaceutical Medicinal Chemistry and Drug Design, Faculty of Pharmacy (Girls), Al-Azhar University, Cairo 11651, Egypt*

Aisha A. Alsfouk − *Department of Pharmaceutical Sciences, College of Pharmacy, Princess Nourah bint Abdulrahman University, Riyadh 11671, Saudi Arabia;* orcid.org/0000-0003-4497-5013

Rehab Sabour − *Department of Pharmaceutical Medicinal Chemistry and Drug Design, Faculty of Pharmacy (Girls), Al-Azhar University, Cairo 11651, Egypt*

Complete contact information is available at: https://pubs.acs.org/10.1021/acsomega.4c10286

Notes

The authors declare no competing financial interest.

■ ACKNOWLEDGMENTS

Acknowledgement to Deanship of Scientific Research and Libraries at Princess Nourah bint Abdulrahman University for funding this research through the research funding program, Grant No. (FRP-1445-4).

■ REFERENCES

(1) Arias, C. A.; Murray, B. E. A new antibiotic and the evolution of resistance. *N. Engl. J. Med.* **2015**, *372*, 1168−1170.

(2) Wagdy, R. A.; Abutaleb, N. S.; Fathalla, R. K.; Elgammal, Y.; Weck, S.; Pal, R.; Fischer, P. D.; Ducho, C.; Abadi, A. H.; Seleem, M. N.; Engel, M.; Abdel-Halim, M. Discovery of 1,2-diaryl-3-oxopyrazolidin-4-carboxamides as a new class of MurA enzyme inhibitors and characterization of their antibacterial activity. *Eur. J. Med. Chem.* **2023**, *261*, No. 115789.

(3) Dunsmore, C. J.; Miller, K.; Blake, K. L.; Patching, S. G.; Henderson, P. J. F.; Garnett, J. A.; Stubbings, W. J.; Phillips, S. E. V.; Palestrant, D. J.; Angeles, J. D.; Leeds, J. A.; Chopra, I.; Fishwick, C. W. G. 2-Aminotetralones: Novel inhibitors of MurA and MurZ. *Bioorg. Med. Chem. Lett.* **2008**, *18*, 1730−1734.

(4) Molina-Lopez, J.; Sanschagrin, F.; Levesque, R. C. A peptide inhibitor of MurA UDP-N-acetylglucosamine enolpyruvyl transferase: The first committed step in peptidoglycan biosynthesis. *peptides* **2006**, *27*, 3115−3121.

(5) Zhang, F.; Graham, J.; Zhai, T.; Liu, Y.; Huang, Z. Discovery of MurA inhibitors as novel antimicrobials through an integrated computational and experimental approach. *Antibiotics* **2022**, *11*, 528.

(6) Baum, E. Z.; Montenegro, D. A.; Licata, L.; Turchi, I.; Webb, G. C.; Foleno, B. D.; Bush, K. Identification and characterization of new inhibitors of the *Escherichia coli* MurA enzyme. *Antimicrob. Agents Chemother.* **2001**, *45*, 3182−3188.

(7) Hrast, M.; Rožman, K.; Jukic, M.; Patin, D.; Gobec, S.; Sova, M. Synthesis and structure-activity relationship study of novel quinazolinone-based inhibitors of MurA. *Bioorg. Med. Chem. Lett.* **2017**, *27*, 3529−3533.

(8) Gautam, A.; Rishi, P.; Tewari, R. UDP-N-acetylglucosamine enolpyruvyl transferase as a potential target for antibacterial chemotherapy: recent developments. *Appl. Microbiol. Biotechnol.* **2011**, *92*, 211−225.

(9) Hrast, M.; Sosič, I.; Sink, R.; Gobec, S. Inhibitors of the peptidoglycan biosynthesis enzymes MurA-F. *Bioorg. Chem.* **2014**, *55*, 2−15.

(10) Rožman, K.; Lešnik, S.; Brus, B.; Hrast, M.; Sova, M.; Patin, D.; Barreteau, H.; Konc, J.; Janežič, D.; Gobec, S. Discovery of new MurA inhibitors using induced-fit simulation and docking. *Bioorg. Med. Chem. Lett.* **2017**, *27*, 944−949.

(11) Arias-Gómez, A.; Godoy, A.; Portilla, J. Functional pyrazolo[1,5-*a*]pyrimidines: Current approaches in synthetic transformations and uses as an antitumor scaffold. *Molecules* **2021**, *26*, 2708.

(12) Castillo, J.-C.; Portilla, J. Recent advances in the synthesis of new pyrazole derivatives. *Targets Heterocycl. Syst.* **2018**, *22*, 194−223.

(13) Ren, L.; Laird, E. R.; Buckmelter, A. J.; Dinkel, V.; Gloor, S. L.; Grina, J.; Newhouse, B.; Rasor, K.; Hastings, G.; Gradl, S. N.; Rudolph, J. Potent and selective pyrazolo[1,5-a]pyrimidine based inhibitors of B-Raf V600E kinase with favorable physicochemical and pharmacokinetic properties. *Bioorg. Med. Chem. Lett.* **2012**, *22*, 1165−1168.

(14) El Sayed, M. T.; Hussein, H. A. R.; Elebiary, N. M.; Hassan, G. S.; Elmessery, S. M.; Elsheakh, A. R.; Nayel, M.; Abdel-Aziz, H. A. Tyrosine kinase inhibition effects of novel Pyrazolo[1,5-a]pyrimidines and Pyrido[2,3-d]pyrimidines ligand: Synthesis, biological screening and molecular modeling studies. *Bioorg. Chem.* **2018**, *78*, 312−323.

(15) (15) Jiang, J. K.; Huang, X.; Shamim, K.; Patel, P. R.; Lee, A.; Wang, A. Q.; Nguyen, K.; Tawa, G.; Cuny, G. D.; Yu, P. B.; Zheng, W.; Xu, X.; Sanderson, P.; Huang, W. Discovery of 3-(4-sulfamoylnaphthyl)pyrazolo[1,5-a]pyrimidines as potent and selective ALK2 inhibitors. *Bioorg. Med. Chem. Lett.* **2018**, *28*, 3356−3362.

(16) Ali, G. M. E.; Ibrahim, D. A.; Elmetwali, A. M.; Ismail, N. S. M. Design, synthesis and biological evaluation of certain CDK2 inhibitors based on pyrazole and pyrazolo[1,5-a] pyrimidine scaffold with apoptotic activity. *Bioorg. Chem.* **2019**, *86*, 1−14.

(17) Hwang, J. Y.; Windisch, M. P.; Jo, S.; Kim, K.; Kong, S.; Kim, H. C.; Kim, S.; Kim, H.; Lee, M. E.; Kim, Y.; Choi, J.; Park, D. S.; Park, E.; Kwon, J.; Nam, J.; Ahn, S.; Cechetto, J.; Kim, J.; Liuzzi, M.; No, Z.; Lee, J. Discovery and characterization of a novel 7-aminopyrazolo[1,5-a]pyrimidine analog as a potent hepatitis C virus inhibitor. *Bioorg. Med. Chem. Lett.* **2012**, *22*, 7297−7301.

(18) Sun, L.; Gao, P.; Zhan, P.; Liu, X. Pyrazolo[1,5-a]pyrimidine-based macrocycles as novel HIV-1 inhibitors: a patent evaluation of WO2015123182. *Expert Opin. Ther. Pat.* **2016**, *26*, 979−986.

(19) Almansa, C.; de Arriba, A. F.; Cavalcanti, F. L.; Gómez, L. A.; Miralles, A.; Merlos, M.; García-Rafanell, J.; Forn, J. Synthesis and SAR of a new series of COX-2-selective inhibitors: Pyrazolo[1,5-*α*]pyrimidines. *J. Med. Chem.* **2001**, *44*, 350−361.

(20) Ayman, R.; Abusaif, M. S.; Radwan, A. M.; Elmetwally, A. M.; Ragab, A. Development of novel pyrazole, imidazo[1,2-b]pyrazole, and pyrazolo[1,5-a]pyrimidine derivatives as a new class of COX-2 inhibitors with immunomodulatory potential. *Eur. J. Med. Chem.* **2023**, *249*, No. 115138.

(21) Hassan, A. S.; Masoud, D. M.; Sroor, F. M.; Askar, A. A. Synthesis and biological evaluation of pyrazolo[1,5-a]pyrimidine-3-

carboxamide as antimicrobial agents. *Med. Chem. Res.* **2017**, *26*, 2909−2919.
(22) Abdallah, A. E. M.; Elgemeie, G. H. Design, synthesis, docking, and antimicrobial evaluation of some novel pyrazolo[1,5-a] pyrimidines and their corresponding cycloalkane ring-fused derivatives as purine analogs. *Drug Des. Devel. Ther.* **2018**, *12*, 1785−1798.
(23) Fouda, A. M.; Abbas, H. S.; Ahmed, E. H.; Shati, A. A.; Alfaifi, M. Y.; Elbehairi, S. I. Synthesis, *in vitro* antimicrobial and cytotoxic activities of some new pyrazolo[1,5-a]pyrimidine derivatives. *Molecules* **2019**, *24*, 1080−1099.
(24) Tellew, J. E.; Lanier, M.; Moorjani, M.; Lin, E.; Luo, Z.; Slee, D. H.; Zhang, X.; Hoare, S. R. J.; Grigoriadis, D. E.; Denis, Y. S.; Fabio, R. D.; Modugno, E. D.; Saunders, J.; Williams, J. P. Discovery of NBI-77860/GSK561679, a potent corticotropin-releasing factor (CRF1) receptor antagonist with improved pharmacokinetic properties. *Bioorg. Med. Chem. Lett.* **2010**, *20*, 7259−7264.
(25) Childress, E. S.; Wieting, J. M.; Felts, A. S.; Breiner, M. M.; Long, M. F.; Luscombe, V. B.; Rodriguez, A. L.; Cho, H. P.; Blobaum, A. L.; Niswender, C. M.; Emmitte, K. A.; Conn, P. J.; Lindsley, C. W. Discovery of Novel Central Nervous System Penetrant Metabotropic Glutamate Receptor Subtype 2 (mGlu 2) Negative Allosteric Modulators (NAMs) Based on Functionalized Pyrazolo[1,5-a]-pyrimidine-5-carboxamide and Thieno[3,2-b] pyridine-5-carboxamide Cores. *J. Med. Chem.* **2019**, *62*, 378−384.
(26) Saqub, H.; Proetsch-Gugerbauer, H.; Bezrookove, V.; Nosrati, M.; Vaquero, E. M.; de Semir, D.; Ice, R. J.; McAllister, S.; Soroceanu, L.; Kashani-Sabet, M.; Osorio, R.; Dar, A. A. Dinaciclib, a cyclin-dependent kinase inhibitor, suppresses cholangiocarcinoma growth by targeting CDK2/5/9. *Sci. Rep.* **2020**, *10*, 18489.
(27) Mekky, A. E. M.; Taha, N. A. S.; Mohammed, N. G.; Hussein, F. R. M.; Abdelfattah, E. H.; Gamal Eldin, A. A.; Abdelsalam, A. A. M.; Sanad, S. M. H. Development of pyrazolo[1,5-a]pyrimidine-based antibacterial agents. *Synth. Commun.* **2023**, *53*, 1053−1068.
(28) Behbehani, H.; Ibrahim, H. M.; Makhseed, S.; Mahmoud, H. Applications of 2-arylhydrazononitriles in synthesis: Preparation of new indole containing 1,2,3-triazole, pyrazole and pyrazolo[1,5-a]pyrimidine derivatives and evaluation of their antimicrobial activities, Europ. *J. Med. Chem.* **2011**, *46*, 1813−1820.
(29) Al-Adiwish, W. M.; Tahir, M. I. M.; Siti-Noor-Adnalizawati, A.; Hashim, S. F.; Ibrahim, N.; Yaacob, W. A. Synthesis, antibacterial activity and cytotoxicity of new fused pyrazolo [1,5-a]pyrimidine and pyrazolo[5,1-c][1,2,4]triazine derivatives from new 5-aminopyrazoles. *Eur. J. Med. Chem.* **2013**, *64*, 464−476.
(30) Abdallah, A. E. M.; Elgemeie, G. H. Design, synthesis, docking, and antimicrobial evaluation of some novel pyrazolo[1,5-a] pyrimidines and their corresponding cycloalkane ring-fused derivatives as purine analogs. *Drug Des., Devel. and Ther.* **2018**, *12*, 1785−1798.
(31) Ismail, M. M. F.; Khalifa, M. M.; El-Sehrawi, H. M. A.; Sabour, R. Design, synthesis and antimicrobial evaluation of new arylazopyrazole and arylazopyrazolo[1,5-*a*]pyrimidine derivatives. *Polycycl. Aromat. Compd.* **2022**, *42*, 2245−2262.
(32) Ismail, M. M. F.; Soliman, D. H.; Farrag, A. M.; Sabour, R. Synthesis, Antitumor Activity, Pharmacophore Modeling and QSAR Studies of Novel Pyrazoles and Pyrazolo [1, 5-a] Pyrimidines against Breast Adenocarcinoma MCF-7 Cell Line. *Int. J. Pharm. Pharm. Sci.* **2016**, *8* (7), 434−442.
(33) Krystof, V.; Cankar, P.; Frysova, I.; Slouka, J.; Kontopidis, G.; Dzubak, P.; Hajduch, M.; Srovnal, J.; de Azevedo, W. F.; Orsag, M.; et al. 4-Arylazo-3,5-Diamino-1H-Pyrazole CDK Inhibitors: SAR Study, Crystal Structure in Complex with CDK2, Selectivity, and Cellular Effects. *J. Med. Chem.* **2006**, *49* (22), 6500−6509.
(34) Sunduru, N.; Agarwal, A.; Katiyar, S. B.; Nishi, N. G.; Gupta, S.; Chauhan, P. M. Synthesis of 2,4,6- Trisubstituted Pyrimidine and Triazine Heterocycles as Antileishmanial Agents. *Bioorg. Med. Chem.* **2006**, *14*, 7706−7715.
(35) Flemming, H. C.; Wingender, J.; Szewzyk, U.; Steinberg, P.; Rice, S. A.; Kjelleberg, S. Biofilms: an emergent form of bacterial life. *Nat. Rev. Microbiol.* **2016**, *14*, 563−575.
(36) Paredes, J.; Alonso-Arce, M.; Schmidt, C.; Valderas, D.; Sedano, B.; Legarda, J.; Arizti, F.; Gómez, E.; Aguinaga, A.; Del Pozo, J. L.; Arana, S. Smart central venous port for early detection of bacterial biofilm related infections. *Biomed. Microdevices* **2014**, *16*, 365−374.
(37) Wu, H.; Moser, C.; Wang, H. Z.; Høiby, N.; Song, Z. J. Strategies for combating bacterial biofilm infections. *Int. J. Oral Sci.* **2014**, *7*, 1−7.
(38) Mondal, H.; Thomas, J.; Amaresan, N. Assay of Hemolytic Activity. *Aquaculture Microbiology* **2023**, 187−189.
(39) Liu, Y.; Breukink, E. The membrane steps of bacterial cell wall synthesis as antibiotic targets. *Antibiotics* **2016**, *5*, 28.
(40) Laddomada, F.; Miyachiro, M. M.; Dessen, A. Structural insights into protein-protein interactions involved in bacterial cell wall biogenesis. *Antibiotics* **2016**, *5*, 14.
(41) Egan, A. J.; Errington, J.; Vollmer, W. Regulation of peptidoglycan synthesis and remodelling. *Nat. Rev. Microbiol.* **2020**, *18*, 446−460.
(42) Vollmer, W.; Blanot, D.; De Pedro, M. A. Peptidoglycan structure and architecture. *FEMS Microbiol. Rev.* **2008**, *32*, 149−167.
(43) Sarkar, P.; Yarlagadda, V.; Ghosh, C.; Haldar, J. A review on cell wall synthesis inhibitors with an emphasis on glycopeptide antibiotics. *Med. Chem. Comm.* **2017**, *8*, 516−533.
(44) Klein, C. D.; Bachelier, A. Molecular modeling and bioinformatical analysis of the antibacterial target enzyme MurA from a drug design perspective. *J. Comput. Aided Mol. Des.* **2006**, *20*, 621−628.
(45) Harras, M. F.; Sabour, R.; Farghaly, T. A.; Ibrahim, M. H. Drug Repurposing Approach in Developing New Furosemide Analogs as Antimicrobial Candidates and Anti-PBP: Design, Synthesis, and Molecular Docking. *Bioorg. Chem.* **2023**, *137*, No. 106585.
(46) Mohammed, H. S.; Ibrahim, M. H.; Abdel-Aziz, M. M.; Ghareeb, M. A. Anti-Helicobacter pylori, anti-biofilm activity, and molecular docking study of citropten, bergapten, and its positional isomer isolated from Citrus sinensis L. leaves. *Heliyon* **2024**, *10*, No. e25232.
(47) Zhang, Z.; Yan, J.; Leung, D.; Costello, P.; Sanghera, J.; Daynard, T.; Wang, S.; Chafeev, M. Pyrazole Compounds. United States Patent US20020042501A1 2002.
(48) Fouda, A. M.; Abbas, H. S.; Ahmed, E. H.; Shati, A. A.; Alfaifi, M. Y.; Elbehairi, S. I. Synthesis, in Vitro Antimicrobial and Cytotoxic Activities of Some New Pyrazolo[1,5-a]pyrimidine Derivatives. *Molecules* **2019**, *24* (6), 1080.
(49) Ismail, M. M. F.; Farrag, A. M.; Harras, M. F.; Ibrahim, M. H.; Mehany, A. B. M. Apoptosis: A target for anticancer therapy with novel cyanopyridines. *Bioorganic Chemistry* **2020**, *94*, No. 103481.
(50) Iftikhar, S.; Khan, S.; Bilal, A.; Manzoor, S.; Abdullah, M.; Emwas, A. H.; Sioud, S.; Gao, X.; Chotana, G. A.; Faisal, A.; Saleem, R. S. Z. Synthesis and evaluation of modified chalcone based p53 stabilizing agents. *Bioorg. Med. Chem. Lett.* **2017**, *27*, 4101−4106.
(51) Ibrahim, M. H.; El Menofy, N. G.; El kiki, S. M.; Sherbiny, F. F.; Ismail, M. M. F. Development of fluorinated nicotinonitriles and fused candidates as antimicrobial, antibiofilm, and enzyme inhibitors. *Arch Pharm. (Weinheim)* **2022**, *355*, No. 2200040.
(52) Bayazeed, A.; Alenazi, N. A.; Alsaedi, A. M. R.; Ibrahim, M. H.; Al-Qurashi, N. T.; Farghaly, T. A. Formazan analogous: Synthesis, antimicrobial activity, dihydrofolate reductase inhibitors and docking study. *J. Mol. Struct.* **2022**, *1258*, No. 132653.
(53) Rodríguez-Tudela, J. L.; Barchiesi, F.; Bille, J.; Chryssanthou, E.; Cuenca-Estrella, M.; Denning, D.; Donnelly, J. P.; Dupont, B.; Fegeler, W.; Moore, C.; Richardson, M.; Verweij, P. E. Method for the determination of minimum inhibitory concentration (MIC) by broth dilution of fermentative yeasts. *Clinical Microbiology and Infection* **2003**, *9*, i−viii.
(54) Antunes, A. L. S.; Trentin, D. S.; Bonfanti, J. W.; Pinto, C. C. F.; Perez, L. R. R.; Macedo, A. J.; Barth, A. L. Application of a feasible method for determination of biofilm antimicrobial susceptibility in staphylococci. *APMIS.* **2010**, *118*, 873−877.

https://doi.org/10.1021/acsomega.4c10286
ACS Omega 2025, 10, 4044−4056

(55) Rossignol, G.; Merieau, A.; Guerillon, J.; Veron, W.; Lesouhaitier, O.; Feuilloley, M. G.; Orange, N. Involvement of a phospholipase C in the hemolytic activity of a clinical strain of Pseudomonas fluorescens. *BMC Microbiol.* **2008**, *8*, 189.

https://doi.org/10.1021/acsomega.4c10286
ACS Omega 2025, 10, 4044−4056